The Theory of SNOM: A novel approach

A. J. Ward, J. B. Pendry
The Blackett Laboratory, Imperial College,
London, SW7 2BZ, UK

July 4, 2021

Abstract

In this paper we consider the application of electromagnetic theory to the analysis of the Scanning Near-field Optical Microscope (SNOM) in order to predict experimentally observable quantities such as the transmission or reflection coefficients for a particular tip-surface configuration. In particular we present the first application of a transfer matrix based calculation to this challenging problem by using an adaptive co-ordinate transformation to accurately model the shape of the SNOM tip.

We also investigate the possibility of increasing the transmitted light through the SNOM tip by introducing a metal wire into the centre of the tip. This converts the tip into a co-axial cable. We show that, in principle, this can dramatically improve the transmission characteristics without having a detrimental effect on the resolution.

1 Introduction

One of the first lessons in optics which is drummed into our heads is that the resolution of any optical instrument is limited, fundamentally, by the wavelength of the light it uses. However, this resolution limit is not an absolute and, in fact, applies only to the image in the far field. Sub-wavelength information can, in principle, be obtained by probing the near field which contains both the propagating modes and evanescent modes bound to the surface of the object. It is these evanescent modes which correspond to sub-wavelength spatial frequencies and so encode the nano-metric detail of the object. So the principle which lies behind near-field imaging techniques is this: find some way to probe the near-field and imaging details smaller than the wavelength becomes feasible.

In the early nineties, Pohl and co-workers at IBM [1, 2], designed a near-field 'optical stethoscope' for imaging at a wavelength of 448nm with a claimed resolution of about $\lambda/20$. Since then, many other groups have built Scanning Near-field Optical Microscopes (SNOM, or sometimes NSOM) along similar lines. A typical, modern SNOM can be described as follows. The surface under investigation is illuminated from above by laser light passing down an optical fibre. The end of the fibre is formed into a taper and the sides of the taper are

coated in about 100nm of a metal, typically aluminium or silver [3], the very end of the tip being left uncoated. In this way apertures can be reliably produced with diameters of $\sim$ 20-500nm. As the tip is scanned over the surface, a shear-force mechanism is used to regulate the tip surface distance [4, 5]. At each point the light transmitted through the sample is collected by a photomultiplier and a complete image built up. Such a device also offers the possibility for performing local, high resolution spectroscopy [6, 7, 8].

Many variations on this basic idea are possible and there are several comprehensive reviews [9, 10]. Possibilities include measuring the reflected rather than the transmitted light, illuminating from below and using the coated fibre tip as a light collector, or even illuminating from below above the critical angle and using an uncoated tip as a nano-scatterer to disrupt the near-field and frustrate total internal reflection [11, 12].

However, if the SNOM is to mature as an analytical tool then theorists have a critical role to play, both in order to interpret correctly the images produced by the microscope, but also to assist in the optimisation of tip and illumination system. Several approaches are possible for solving the problem of the electromagnetic scattering between tip and surface, amongst those suggested have been finite difference time domain schemes and boundary matching methods. The former usually require a super-computer to handle a problem as complex as this. The latter, which expands the fields in each region in some suitable complete basis set and matches the fields at the boundaries, faces difficulties when handling regions of irregular shapes, which are needed for a realistic description of the tip. However, one group have completely dominated the theory of the near-field microscope by introducing an iterative Green's function based method [13, 14]. Using this method Girard *etal.* have been able to simulate images produced by reflection microscopes scanning over a range of dielectric and metal objects.

2 A novel approach

However, despite the sophistication of Girard's method it does rely on a real space discretisation in order to represent both object and tip. For an accurate description of the tip this is can be a serious restriction, especially if we are restricted to a regular, Cartesian grid. The problem is this: in reality the surface of the tip is a cone or paraboloid shape with a smooth surface, discretisation leads to a surface covered in steps, the size of which depends on the mesh size. The presence of these steps will result in additional scattering from the surface of the tip and may reduce the accuracy of the calculation especially if the size of the discretisation mesh is large. The only way to reduce the error is to use more mesh points leading to larger, slower calculations.

We can, however, tackle the SNOM problem from a slightly different angle which helps us to overcome these problems. The idea is to perform the discretization in a co-ordinate system which follows the shape of the tip itself. While, in principle, the construction of such an adaptive, discrete mesh may

seem a horribly complex task, in practise this is not so. This is because of a useful result which allows us to factorise the problem into two parts. This result, which is derived in detail elsewhere [15], allows us to transfer all the details of the mesh geometry into an effective, tensorial permittivity and permeability ($\hat{\varepsilon}^{\alpha\beta}$, $\hat{\mu}^{\alpha\beta}$). Now we need only perform the discretization on a regular, cartesian mesh and then map that onto the adaptive mesh by introducing the appropriate $\hat{\varepsilon}$ and $\hat{\mu}$.

How do Maxwell's equations appear in the adaptive co-ordinate system? The result is surprisingly simple. Let q_1, q_2, q_3 be the co-ordinates in our adaptive co-ordinate system and let the unit vectors $\mathbf{u}_1, \mathbf{u}_2, \mathbf{u}_3$ point along the generalised q_1, q_2, q_3 axes. In this system Maxwell's equations become:

$$\nabla_q \times \hat{\mathbf{E}} = -\mu_0 \hat{\mu}\, \partial \hat{\mathbf{H}}/\partial t \tag{1}$$

$$\nabla_q \times \hat{\mathbf{H}} = +\varepsilon_0 \hat{\varepsilon}\, \partial \hat{\mathbf{E}}/\partial t$$

where,

$$\hat{\varepsilon}^{\alpha\beta} = \varepsilon\; g^{\alpha\beta}\, |\mathbf{u_1} \cdot (\mathbf{u_2} \times \mathbf{u_3})|\; \frac{Q_1 Q_2 Q_3}{Q_\alpha Q_\beta}$$

$$\hat{\mu}^{\alpha\beta} = \mu\; g^{\alpha\beta}\, |\mathbf{u_1} \cdot (\mathbf{u_2} \times \mathbf{u_3})|\; \frac{Q_1 Q_2 Q_3}{Q_\alpha Q_\beta} \tag{2}$$

$$\hat{E}_\alpha = Q_\alpha E_\alpha \qquad \hat{H}_\alpha = Q_\alpha H_\alpha$$

and,

$$Q_\alpha^2 = \left(\frac{\partial x}{\partial q_\alpha}\right)^2 + \left(\frac{\partial y}{\partial q_\alpha}\right)^2 + \left(\frac{\partial z}{\partial q_\alpha}\right)^2 \tag{3}$$

$$\mathbf{g}^{-1} = \begin{bmatrix} \mathbf{u_1} \cdot \mathbf{u_1} & \mathbf{u_1} \cdot \mathbf{u_2} & \mathbf{u_1} \cdot \mathbf{u_3} \\ \mathbf{u_2} \cdot \mathbf{u_1} & \mathbf{u_2} \cdot \mathbf{u_2} & \mathbf{u_2} \cdot \mathbf{u_3} \\ \mathbf{u_3} \cdot \mathbf{u_1} & \mathbf{u_3} \cdot \mathbf{u_2} & \mathbf{u_3} \cdot \mathbf{u_3} \end{bmatrix} \tag{4}$$

Notice that in general $\mathbf{u}_\alpha$, Q_α and $g^{\alpha\beta}$ as well as ε and μ will be functions of position.

3 Details of our calculations

We wish to calculate the transmitted intensity through a given tip and surface configuration and to this end we shall employ a transfer matrix method familiar to the theory of photonic band gap materials [16]. Put simply this involves integrating the electric and magnetic fields from one side of the system to the other by means of a *transfer matrix* which relates the fields in one layer of the mesh to the fields in the next layer.

As a first attempt calculation we will try to simplify the problem as much as possible. By exploiting the obvious cylindrical symmetry of the tip we can reduce the problem from a three dimensional to a two dimensional one. The other major simplification we can impose is in the boundary conditions. By imposing

cylindrical symmetry we have confined the calculation to a cylindrical region of space containing both tip and surface. As usual for a transfer matrix method we can send an incident wave into the system from either end of the cylinder and find the transmission and reflection coefficients [17] but we must specify the boundary conditions for the fields at the cylinder's edge (see figure 1). The simplest form these boundary conditions can take is if we enclose the cylinder with a perfect metal, in other words we set the fields to zero at the boundary. This is not a trivial approximation to make, a much better solution would be to expand the fields outside the scattering region in some complete basis set and match the fields at the boundary, but it is not a foolish approximation either. As long as the wavefield does not have a sizable magnitude at the boundary and remains tightly localised between the tip and sample, as we might expect it to, then the choice of boundary conditions should not have a major effect on the results.

3.1 An analytic form for the tip

Our next choice is that of the discretisation mesh itself for this will determine the shape of the tip which we model. Ideally, we wish to specify the mesh geometry by means of an analytic function – this will greatly simplify the process of defining the effective permittivity and permeability, $\hat{\varepsilon}$ and $\hat{\mu}$, which will contain all the information about the co-ordinate system. We also need to include sufficient parameters in the chosen function to allow us to fine tune the shape of the tip.

One possible form for the mesh is this:

$$r = a\,IR + \frac{1}{2}\left[1 - \cos\left(\frac{2\pi(IZ-1)}{IZ_{max}-1}\right)\right]\{\delta - a\}IR\left(1 - \frac{IR}{IR_{max}}\right)^{\alpha} \tag{5}$$

$$\theta = b\,I\Theta \tag{6}$$

$$z = c\,IZ \tag{7}$$

where IR, $I\Theta$ and IZ are the discrete variables which label each point on the mesh. This form contains five free parameters. The first three a, b, c describe an undistorted mesh. That is to say if $\delta = a$ and $\alpha = 1$ the mesh defined is just discrete cylindrical polar co-ordinates with a radial spacing of a, angular spacing of b and a spacing c in the z-direction. The other two parameters α and δ control the distortion of this cylindrical mesh into a kind of hour glass shape; δ defines the minimum radial distance between points at the centre of the mesh and α controls how tightly the other co-ordinate lines bunch in at the centre. Figure 2 shows the shape of the co-ordinate lines for a typical choice of parameters.

The tip itself can now be defined by assigning the dielectric constant at each point in the mesh. The tip and substrate are glass, $\varepsilon = (2.16, 0.0)$ the tip is coated with a 90nm layer of aluminium $\varepsilon = 1 - \omega_p^2/\omega(\omega + i\gamma)$ with $\omega_p = 15.1$eV and $\gamma = 0.27$eV. The very end of the tip is not coated and this forms the aperture. A layer of metal around the top of the tip prevents stray light from

the source leaking around the side of the tip. Any object we wish to image can be introduced by changing the dielectric constant just above the surface. Figure 3 shows how the metal coating layer, substrate and object fit onto the distorted co-ordinate system.

4 Results

We will want to make comparisons between different tip designs to see if we can suggest ways to improve the utility of the near-field microscope. In order to do this we shall need some way to estimate the resolution of a given microscope configuration as well as to calculate the transmitted or reflected signal. One way to test the resolution is to compare the signals for two similar objects. Ideally, we would like to calculate the transmission for the tip in arbitrary positions above an arbitrary object and in this way build up a complete image of the object. Unfortunately, we have constrained ourselves somewhat by insisting upon cylindrical symmetry so this is not possible. The only choices available to us for the objects under the tip are rings and discs with the tip sitting directly above their centre. This is made clear in figure 4. Fortunately this is enough to get an estimate of the resolution, as we can compare a ring and a disc of the same outer radius to see whether we can detect the presence of the hole at the centre of the ring.

Figures 5 to 7 show comparisons between transmission coefficients for ring and disc objects for three different tip apertures, given a fixed incident wave of frequency 2.5eV. The objects are made of the same glass as the substrate, 54nm high and the tip-object separation is fixed at 36nm. Each graph gives the transmission against the outer radius of the object. The inner radius of the ring is a few nanometres smaller than the outer radius. Strictly, the outer radius is one radial mesh point larger than the inner radius so, because the mesh points are more closely packed at the centre, the difference increases as the size of the object increases.

As the aperture decreases the overall magnitude of the transmission coefficient is reduced, from around 10^{-7} for an aperture radius of 48nm down to about 6×10^{-9} for a 25nm aperture. Reducing the aperture further proved difficult as the magnitude of the transmission coefficient is reduced so much that the variations in it become comparable with the rounding errors in the calculation.

4.1 Improving the design: Coaxial tips

In order to get a high resolution, clearly what is required is as small an aperture as possible. However, because all the guided modes of the tip run into cut-off once the diameter is smaller than the wavelength, small apertures come at the price of a very small transmitted signal. This is borne out by the results in the previous section, where the transmission for an aperture of 25nm is about two orders of magnitude down on the transmission for a 48nm aperture.

However there is, in principle, a way to overcome this problem. Inserting a wire into the centre of the tip would convert the metal clad waveguide into a tapered coaxial cable. The coax is well known to have a different kind of guided mode called the TEM mode [18] arising from the different boundary conditions satisfied at the centre. This mode has a free space like dispersion with no cut-off and so will propagate down the cable for any value of its radius offering the possibility of delivering a much higher photon flux to the end of the tip.

There are one or two potential problems with using a coaxial tip in a microscope, of course. The main one is the fear that the extra absorption caused by introducing a lossy metal into the centre of the guide would negate any gain given by the new mode, especially as the field distribution in the TEM mode behaves like $1/r$ so is largest along the central wire. We do our best to minimise this by limiting the central wire only to the very end of the tip, where the radius has fallen below the cut-off point. We also try to maintain a uniform impedance along the coaxial part by ensuring that the central wire tapers in the same proportions as the rest of the tip. The other constraint we must be careful with is not to make the wire too thin. Once the radius of the wire is much less than the skin depth it will no longer be effective.

In order to optimise the transmitted power through the coaxial tip we sought a compromise between the lack of cut-off in the TEM mode and the increased absorption due to the central wire. To this end we varied the length of wire inside the end of the tip and found the optimum value to be 180nm. The radius of the wire at the very end of the tip is 6.8nm. We then repeated the previous calculations, the results being shown in figures 8 to 10.

Comparing figures 8 to 10 to figures 5 to 7 shows the improvement in the magnitude of the transmission when using the new tip. For the 35nm aperture the improvement is about two orders of magnitude, falling to about one order of magnitude for the 25nm aperture. The general increase in signal strength has allowed us to perform the calculation for a smaller aperture than before, of only 17nm radius. Also it is clear that the resolution for the coaxial tip is equal to if not slightly better than the conventional tip. The shape of the graphs at larger object radii is clearly much flatter than for the normal tip. We expect the fields to be strongly confined in the region between tip and sample. The more tightly the fields are confined, the smaller the spot on the surface illuminated and so the less effect adding dielectric material to the object at large radii has on the transmission. This would seem to suggest fields more tightly confined for the coaxial tip compared to the normal one.

Figure 11 shows the transmission coefficient as a function of aperture radius for both types of tip and shows that for the range of apertures from about 65nm to 20nm the coaxial design offers significant improvement.

5 Conclusions and future work

In this paper we have presented the first attempt to apply the transfer matrix method to calculate the properties of the near-field optical microscope. We

have calculated the transmission coefficient for a range of aperture radii as well as estimating the resolution by comparing the transmission data for slightly different objects under the tip.

Whilst our calculations may lack the sophistication of others that have been performed in this field, ours are the first, to the best of our knowledge, to use an adaptive mesh scheme to follow accurately the shape of the tip. There is no reason, in principle, why this co-ordinate transformation cannot be applied to other methods. Many other techniques such as Girard's method or the Finite difference time domain method rely on a real space discretisation at some point and so could directly benefit from the adaptive mesh we have developed here. In the future we also hope to remove the constraint of working within cylindrical symmetry and so calculate images of objects directly.

We have also presented the first calculations for a near-field microscope with a coaxial tip. These results clearly show the potential for such a tip to enhance the magnitude of the transmitted signal even at very small aperture sizes. The only theoretical limit on the size of such a tip is the need for the central wire to have a diameter larger than the skin depth.

Experimentally, some progress has been made towards realising such a tip. Fischer *etal.* [19] investigated the properties of a conical glass tip manufactured with a silver wire taper placed at the centre. However, difficulties in obtaining an unbroken metal core prevented him from using the tip for imaging. More recently, he has suggested a tetrahedral tip [20] coated with metal except for one edge as an alternative which may offer the advantages of the coaxial design but without the manufacturing difficulties. It is hoped that calculations of the kind outlined here can be of use in analysing the merits of alternative SNOM designs such as these.

References

[1] Pohl D W, Denk W, Lanz M, 1984, *Appl. Phys. Lett.* **44** 651.

[2] Dürig U, Pohl D W, Rohner F, 1986, *J. Appl. Phys.* **59** 3318.

[3] Betzig E, Trautman J K, Harris T D, Weiner J S, Kostelak R L, 1991, *Science* **251** 1468.

[4] Toledo-Crow R, Yang P C, Chen Y, Vaez-Iravani M, 1992, *Appl. Phys. Lett.* **60** 2957.

[5] Betzig E, Finn P L, Weiner J S, 1992, *Appl. Phys. Lett.* **60** 2484.

[6] Trautman J K, Macklin J J, Brus L E, Betzig E, 1994, *Nature* **369** 40.

[7] Xie S X, Dunn R C, 1994, *Science* **265** 361.

[8] Ambrose W P, Goodwin P M, Martin J C, Keller R A, 1994, *Science* **265** 364.

[9] Courjon D, Baida F, Bainier C, Van Labeke D, Barchiesi D, 1995, 'Photons and Local Probes' 59-77, Ed. Marti O, Möller R, Kluwer Academic Publishers.

[10] Courjon D, Bainier C, 1994, *Rep. Prog. Phys.* **57** 989.

[11] Courjon D, Sarayeddine K, Spajer M, 1989, *Optics Commun.* **71** 23.

[12] Reddick R C, Warmack R J, Ferrell T L, 1989, *Phys. Rev. B* **39** 767.

[13] Martin O J F, Girard C, Dereux A, 1995, *Phys. Rev. Lett.* **74** 526.

[14] Girard C, Dereux A, 1996, *Rep. Prog. Phys.* **59** 657.

[15] Ward A J, Pendry J B, 1996, *J. Mod. Optics* **43** 773.

[16] Pendry J B, MacKinnon A, 1992, *Phys. Rev. Lett.* **69** 2772.

[17] Pendry J B, 1994, *J. Mod. Optics* **41** 209.

[18] Jackson J D, Classical Electrodynamics, 1975, Wiley, 339-342.

[19] Fischer U C, Zapletal M, 1992, *Ultramicroscopy* **42**, 393.

[20] Koglin J, Fischer U C, Brzoska K D, Göhde W, Fuchs H, 1995, 'Photons and Local Probes' 79-92, Ed. Marti O, Möller R, Kluwer Academic Publishers.

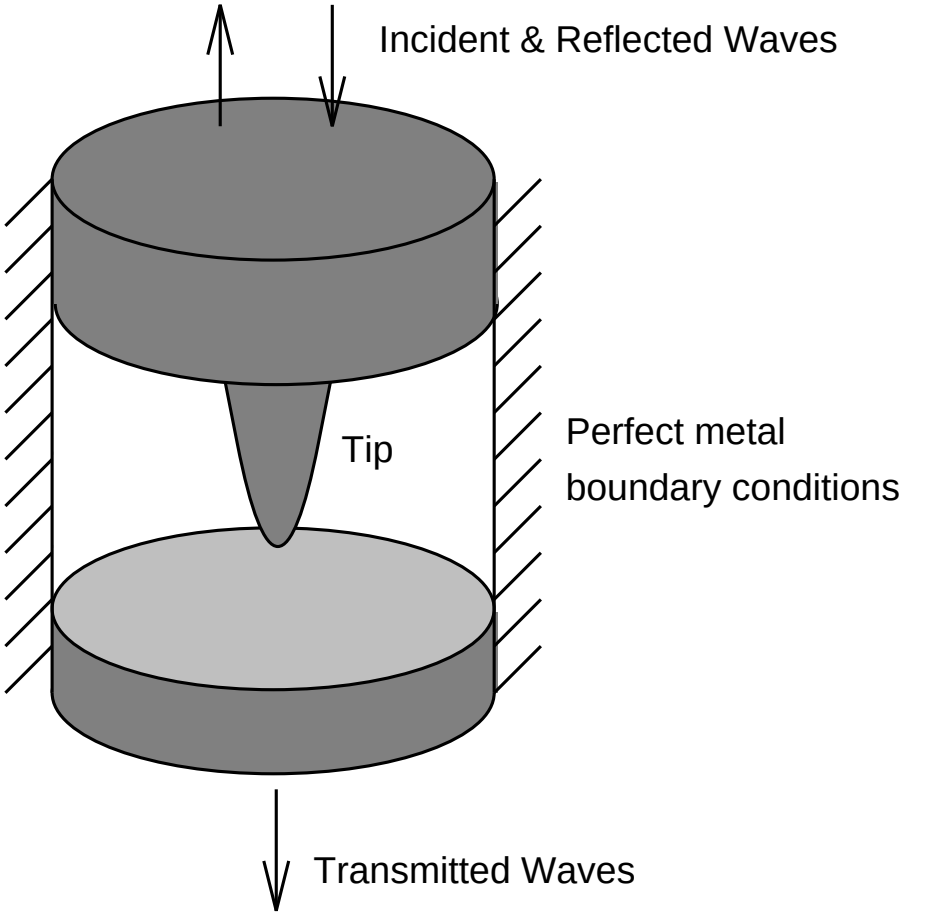

Figure 1: The tip-surface scattering system is contained within a cylinder. Waves can be incident from top or bottom, but the boundary conditions at the side must be specified.

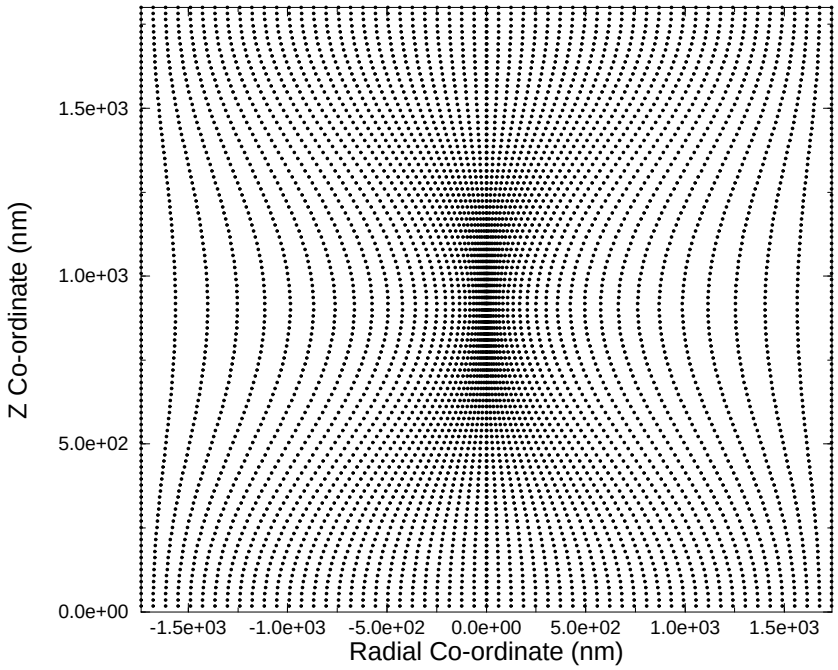

Figure 2: A typical mesh used to represent the SNOM tip.

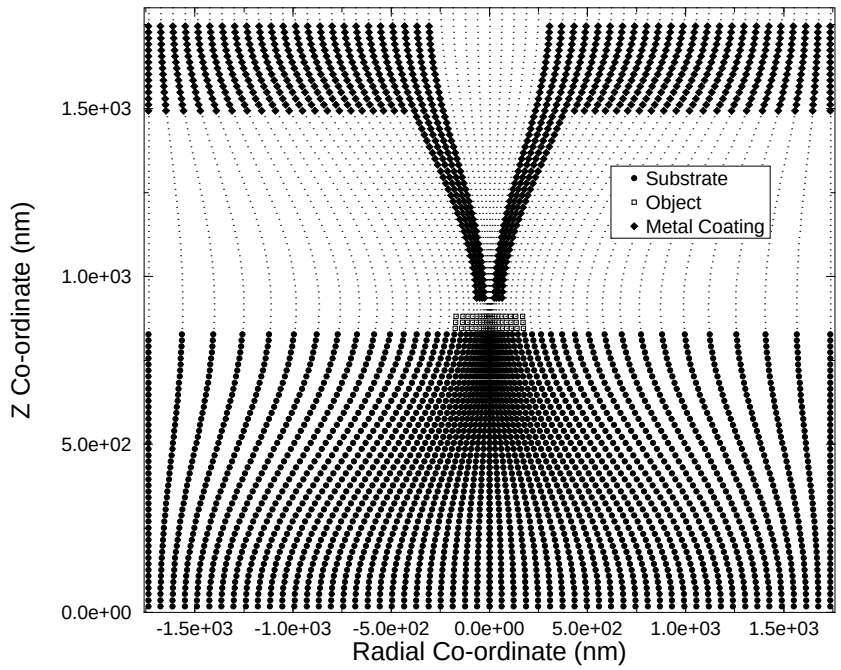

Figure 3: The mesh shaded to indicate the presence of the metal coating the tip (Diamonds), the substrate (circles) and the object being studied (squares)

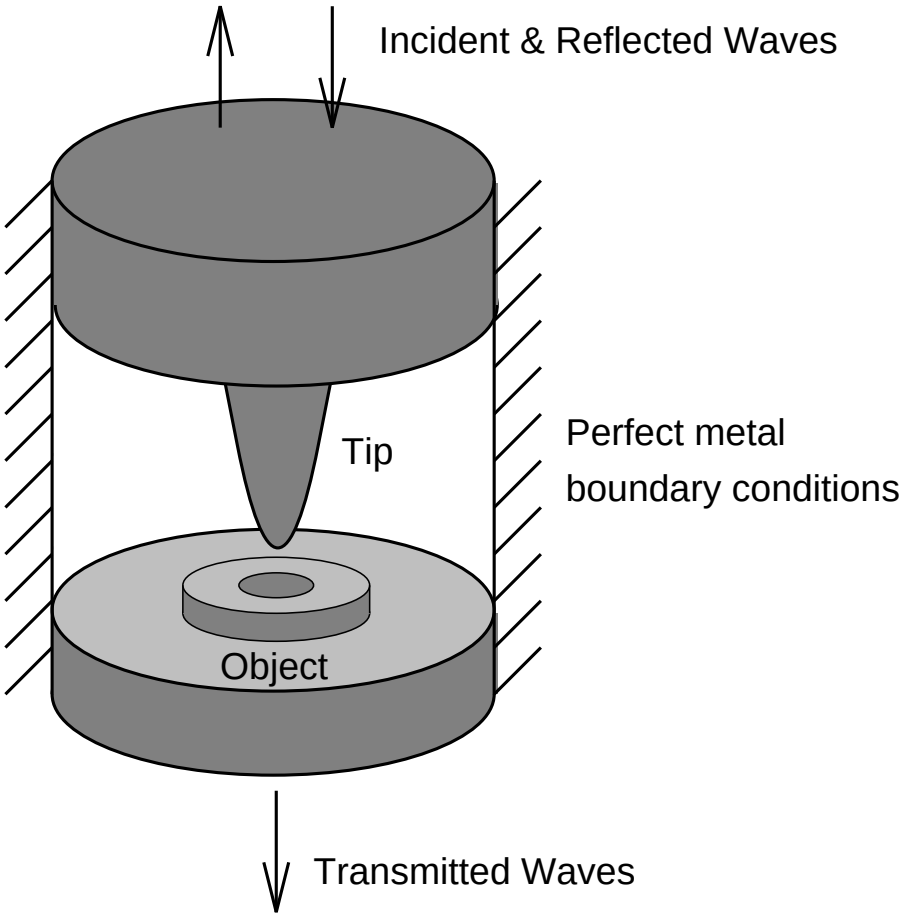

Figure 4: Disc or ring objects (ring shown) can be placed under the tip.

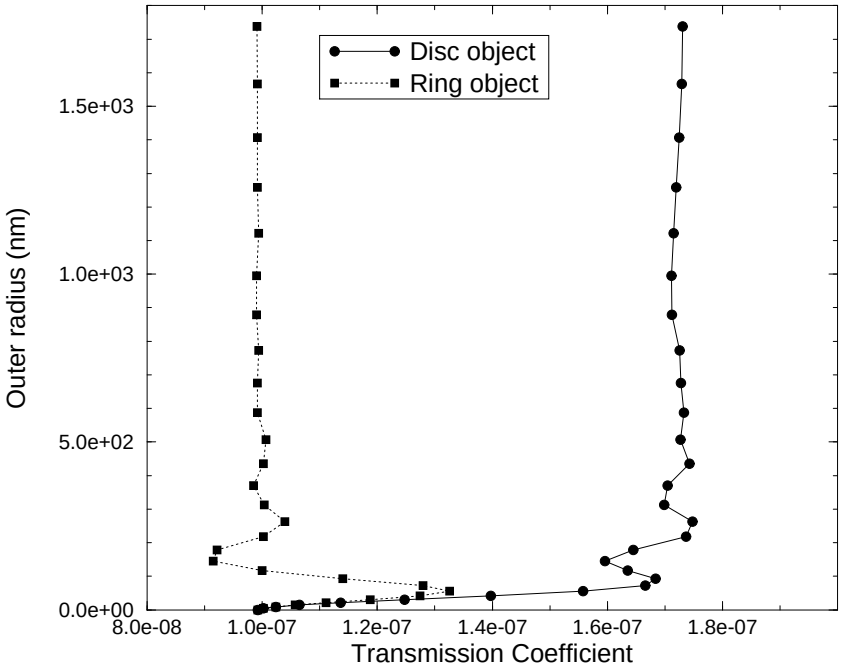

Figure 5: Comparison of transmission coefficients for ring and disc objects. Aperture radius 48nm

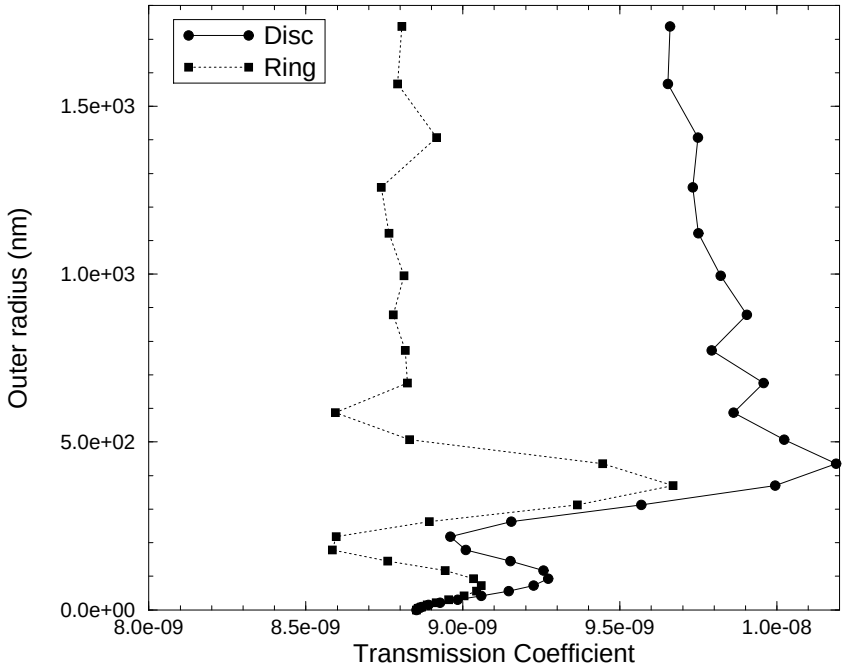

Figure 6: Comparison of transmission coefficients for ring and disc objects. Aperture radius 35nm

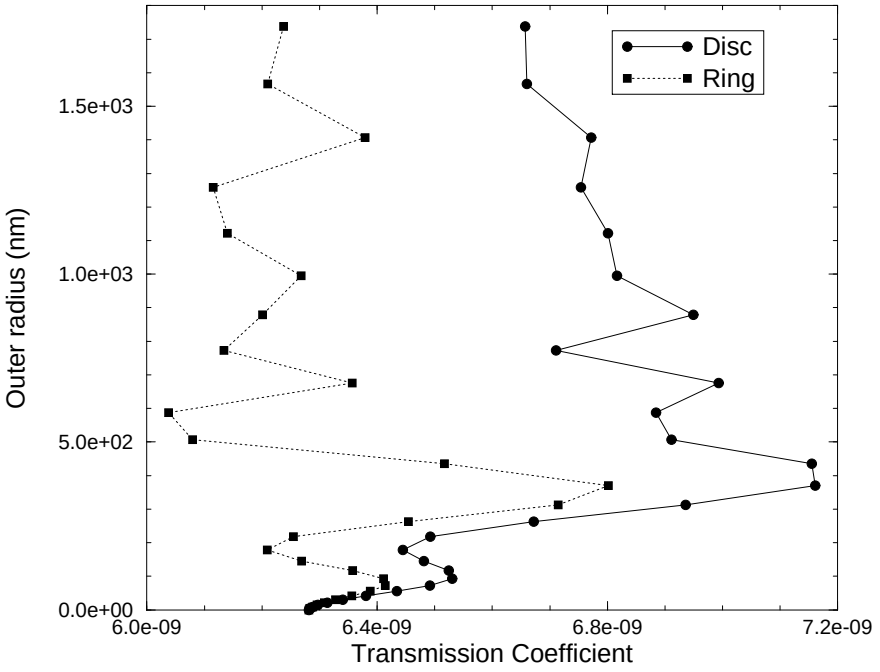

Figure 7: Comparison of transmission coefficients for ring and disc objects. Aperture radius 25nm

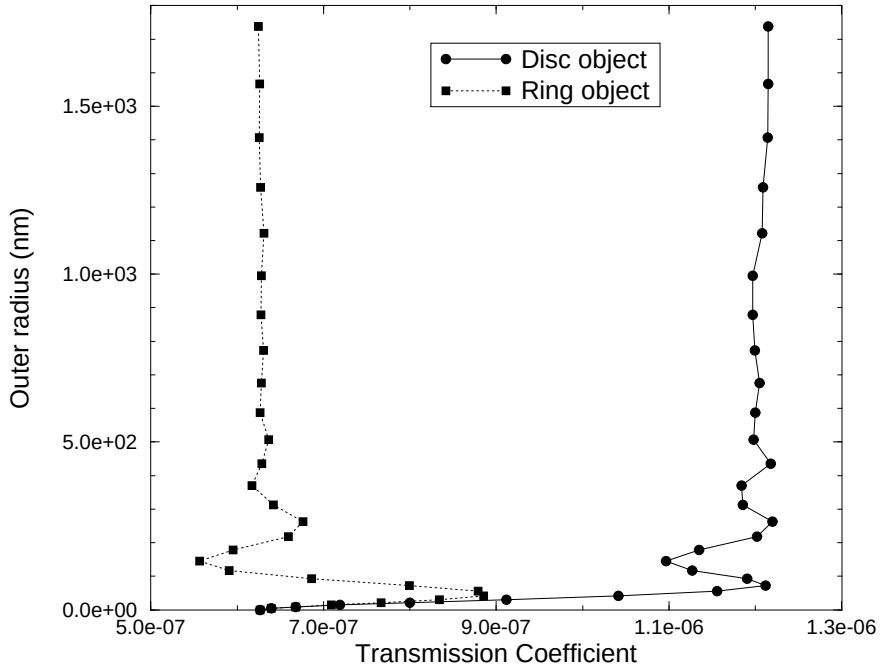

Figure 8: Comparison of transmission coefficients for ring and disc objects. New Coaxial tip of aperture 35nm

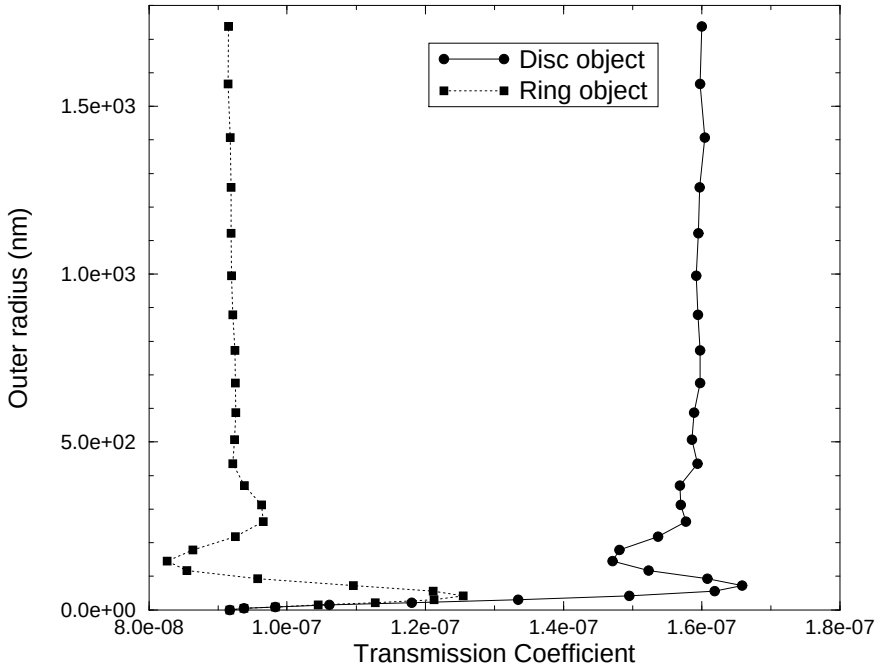

Figure 9: Comparison of transmission coefficients for ring and disc objects. New Coaxial tip aperture 25nm

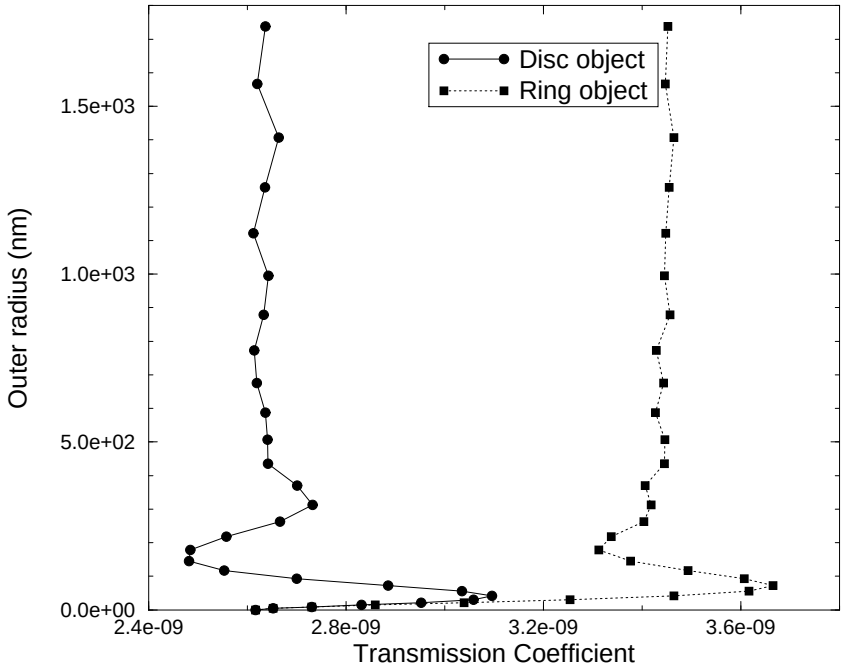

Figure 10: Comparison of transmission coefficients for ring and disc objects. New Coaxial tip aperture 17nm

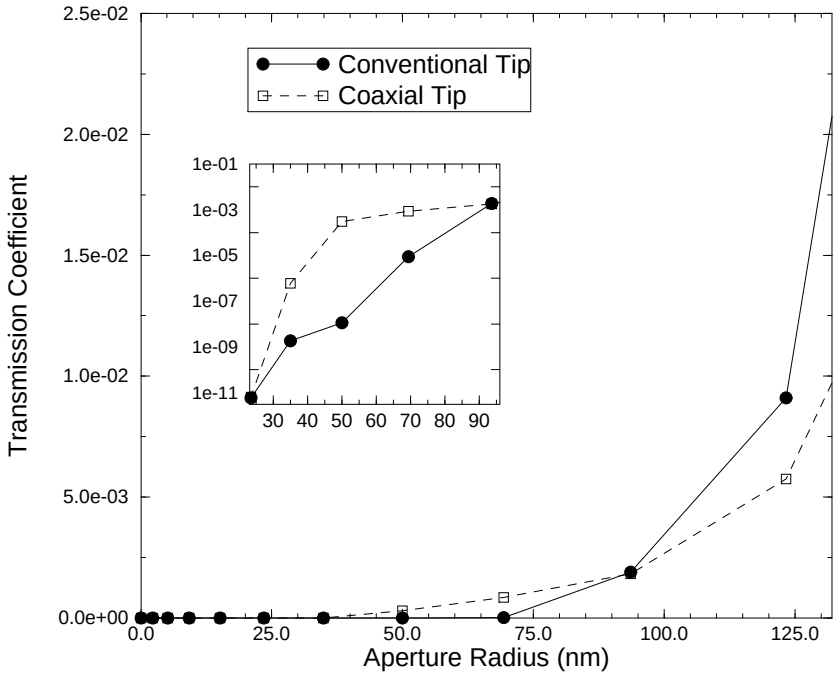

Figure 11: Transmission coefficient against aperture radius for the conventional and coaxial tips. The inset is a plot of the log of the transmission against radius in the critical region